Asian Journal of Chemistry; Vol. 25, No. 11 (2013), 6167-6172

ASIAN JOURNAL OF CHEMISTRY

http://dx.doi.org/10.14233/ajchem.2013.14299

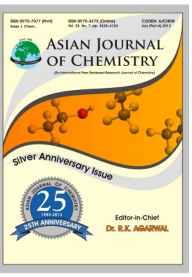

Photoelectrochemical Properties and Its Application of Nano-TiO_2/Boron-doped Diamond Heterojunction Electrode Material

Yanhe Han[1,*], Xiuli Ruan[2], Jiaqing Chen[1], Haimin Zhang[3], Huijun Zhao[3] and Shanqing Zhang[3]

[1]Department of Environmental Engineering, Beijing Institute of Petrochemical Technology, 19 Qingyuan North Road, Daxing District, Beijing 102617, P.R. China
[2]Chinese Research Academy of Environmental Sciences, Da Yang Fang Street No.8, An Wai, Beijing 100012, P.R. China
[3]Griffith School of Environment, Gold Coast Campus, Griffith University, QLD 4222, Australia

*Corresponding author: Tel./Fax: +86 10 82192291; E-mail: hanyanhe@bipt.edu.cn; hanyanhe@126.com

(*Received*: 12 July 2012; *Accepted*: 30 April 2013) AJC-13427

Like titanium dioxide (TiO_2), boron-doped diamond (BDD) is one of the most popular functional materials in recent years. In this work, TiO_2/BDD heterojunction electrodes were prepared by dip-coating TiO_2 nanoparticles onto BDD electrodes. XRD patterns of these electrodes suggest that the mixed-phase TiO_2/BDD heterojunction electrode with anatase and rutile can be obtained at 700 ºC, named as mixed-phase TiO_2/BDD electrode. However, the TiO_2/BDD heterojunction electrode prepared at 450 ºC has only anatase phase TiO_2, named as pure-anatase TiO_2/BDD electrode. SEM images indicate that TiO_2 nanoparticles with *ca.* 20 nm were both immobilized continuously and uniformly onto the BDD electrode whether at 700 ºC or 450 ºC. The photoelectrocatalytic activity of mixed-phase TiO_2/BDD electrode is 3-fold of that obtained at pure-anatase TiO_2/BDD electrode, indicating that mixed-phase TiO_2/BDD electrode is more effective to use to degrade and/or detect the organic compounds. Comparing with the TiO_2/ITO electrode, the TiO_2/BDD electrode presents an excellent chemical stability. The detection of glucose and KHP in the solution indicates that the steady-state net photocurrent in the range of concentration monitored presents superiorly linear relationship to the concentration of glucose and KHP. Therefore, the mixed-phase TiO_2/BDD electrode may be used as a high effective sensing material for the detection of organic compounds.

Key Words: TiO_2/BDD heterojunction electrode, Photoelectrocatalysis, Sensor, Chemical stability.

INTRODUCTION

Boron-doped diamond (BDD) is one of the most promising advanced electrode materials in the field of electroanalysis, because it has a very low background current and noise signals, a wide potential window, a high mechanical strength and corrosion resistance (even being anodic polarized in acidic solutions) and a high resistance to deactivation by impurities and long term response stability[1-4]. These superior characteristics benefit its practical application, specially electrochemical reactions occurring at all extreme environments, when the BDD film was used directly as an electrode or selected as a substrate for combining with other materials[5]. In particular, boron doping makes it a *p*-type semiconductor as well as conductive at room temperature[6,7].

Owing to the excellent photocatalytic activity and superior oxidation ability, TiO_2 photocatalyst has been applied to the fields of water purification/sterilization[8], wastewater treatment[9,10] and environmental detection[11], since Fujishima and Honda discovered the photocatalytic splitting of water on TiO_2 electrodes[12]. A main attraction of such photocatalyst is due to the superior oxidative power of photogenerated holes, high activity radicals and other active oxygen species that can readily degrade a wide spectrum of organic compounds[13-16]. Although the effectiveness has been demonstrated, this technology suffered serious hurdles for practical applications due to poor quantum yield and difficult separation of photogenerated electrons and photogenerated holes[17]. Immobilizing TiO_2 onto a conducting substrate can eliminate the requirement of post-separation, enables the recycle utilization of catalyst and allows to improve the photocatalytic efficiency by suppressing photoelectron/hole recombination. Furthermore, TiO_2 catalyst exhibit *n*-type semiconductor properties[18]. Therefore, the incorporation of *n*-type TiO_2 with the *p*-type BDD can form a heterojunction, which acts as an internal electrostatic potential in the space charge region to facilitate efficient separation of the photoinduced charge carriers[19]. This is an added advantage compared with other substrates, such as ITO and metal. Recently, some researchers have recently prepared the TiO_2/BDD heterojunction systems to photocatalytically or photoelectrocatalytically decompose the pollutants in solution. Manivannan *et al.*[19] reported that the photoelectrocatalytic oxidation of ethanol in acidic solution was investigated using TiO_2/BDD system as the electrode, depositing nanometre-sized TiO_2 particles onto the BDD electrode by electrochemical method. Qu *et al.*[20] investigated the photoelectrocatalytic degradation of acid orange II and 2,4-dichlorophenol using TiO_2/BDD electrode, exhibiting high photoelectroncatalytic activities. Quan and co-workers used the TiO_2/BDD heterojunction to investgate the photocatalytic properties at simultaneously presence of reactive yellow and hexavalent chromium[5]. However, to the best of our knowledge, the photoelectrochemical detection of organic compounds by TiO_2/BDD heterojunction electrode has not been explored.

The objective of this work is to prepare TiO_2/BDD heterojunction electrodes with robust photoelectrocatalytic activity and high chemical stability for the detection of organic compounds. The preparation, characterization and photoelectrocatalytic properties of TiO_2/BDD heterojunction electrode and their application for detection of organic compounds were carried out in this study. Glucose and KHP were selected as organic substrate to be detected, because they are representing weak and strong adsorptive compounds on TiO_2, respectively.

EXPERIMENTAL

Boron-doped diamond (BDD) electrodes with resistivity of 0.1 Ω cm were purchased from CSEM (Switzerland). All chemicals used in this work were of analytical reagent and used as received. All solutions were prepared using high purity deionized water (> 18 MΩ cm).

Preparation of TiO_2/BDD electrodes: Aqueous TiO_2 colloid was prepared by hydrolysis of titanium *n*-butoxide according to the method described in our work[21]. The resultant colloidal solution contains *ca.* 60 g dm^{-3} of TiO_2 solid with particle sizes ranging from 8-10 nm. Carbowax (30 % w/w based on the solid weight of the TiO_2 colloid) was added to increase the porosity of the final TiO_2 film. The BDD electrode was pre-treated by heated aqua regia and H_2O_2 solution and then rinsed with distilled water to remove the surface oxides formed during the acid washing. After pretreatment, the BDD slides were dip-coated in the TiO_2 colloidal solution. The prepared electrodes were then calcined at 450 ºC in air for 2 h, or sintered at 700 ºC in argon atmosphere for 2 h after the carbowax was removed at 450 ºC in air for 0.5 h. And TiO_2/ITO electrodes were also prepared similarly without the aqua regia pretreatment.

The photoelectrocatalytical experiments were performed at room temperature in a three-electrode electrochemical cell with a quartz window for illumination. The working electrode surface area exposed to solution was a circle with diameter of 6 mm, which is the photoelectrochemical reaction area. Platinum mesh and Ag/AgCl (3 M NaCl) electrode were used as the auxiliary and reference electrodes, respectively. Light illumination was achieved with a 150 W Xenon arc lamp light source with focusing lenses (HF-200w-95). To minimize sample heating from the infrared fraction of the source, the light beam was passed through an UV-band pass filter (UG-5, Schott) prior to illuminating the electrode surface. The light intensity was measured with a UV-irradiance meter (UVA, Instruments of Beijing Normal University). A voltammograph (CV-27, BAS) was used for application of potential bias in the photoelectrolysis and linear potential sweep experiments. The TiO_2 film surface morphology and an estimate of the surface porosity were obtained using SEM on the JEOL JSM-6300 F field emission scanning electron microscopy (FESEM, Tokyo, Japan). X-Ray diffractometry was performed with a Philips PW1050 diffractometer using CuK_α radiation.

RESULTS AND DISCUSSION

It was commonly considered that the anatase phase of TiO_2 can be obtained at 450 ºC. The mixed anatase and rutile phases were attained only when the temperature was over 700 ºC[17]. However, it was found that the BDD was oxidated at 700 ºC in the air. Therefore, the TiO_2/BDD electrodes were calcined under different conditions. One was at 450 ºC in the air and the other was at 700 ºC in the protective atmosphere of argon. The SEM images and the XRD patterns of TiO_2/BDD calcined under the two conditions and that of original BDD were showed in Fig. 1. Fig. 1a-b show the FESEM images surface morphology of as-prepared TiO_2/BDD electrode at 450 and 700 ºC, respectively. And the FESEM iamge of cross-section showed in Fig. 1c. Fig. 1a-b indicate that the TiO_2 film distribute continuously and uniformly on BDD electrode in both temperature 450 ºC and 700 ºC. The sizes of TiO_2 particles are in the range of 10-20 nm. Fig. 1c suggests that typical morphology and nanostructure of BDD were well maintained. In other words, the BDD was not damaged by the above sintering treatments and the aqua regia washing process. The rough and uneven in nanoscale structures are beneficial for the immobilization of the TiO_2 film.

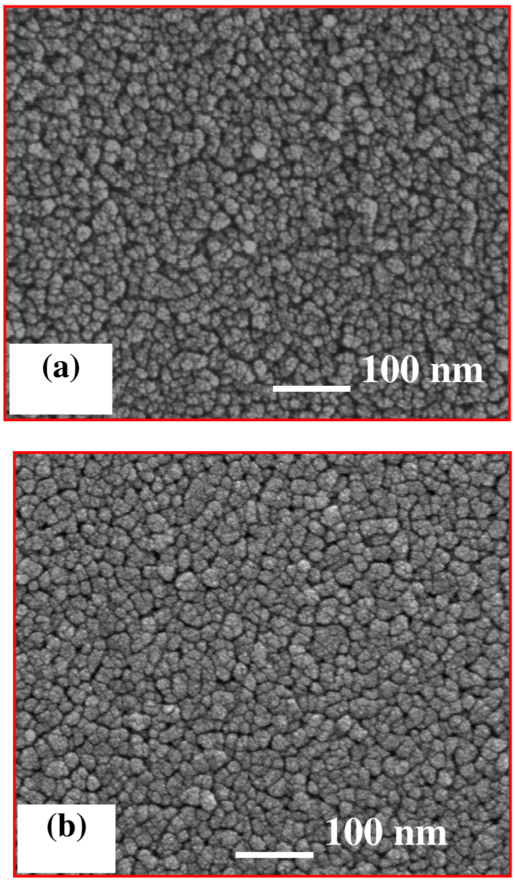

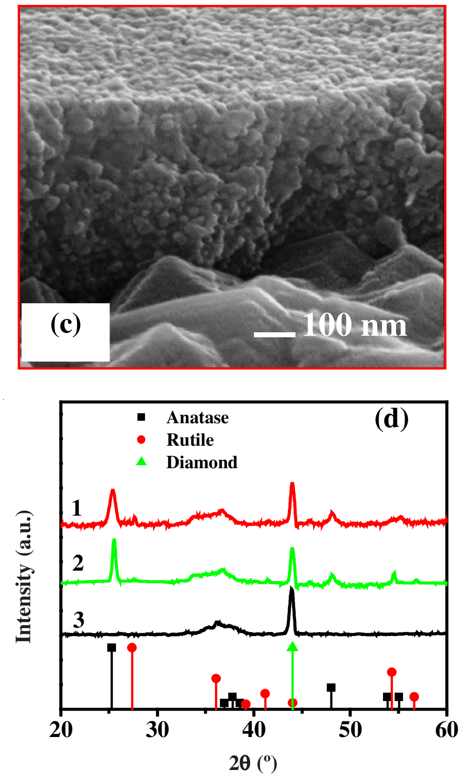

Fig. 1. (a) and (b) are SEM images of the TiO$_2$/BDD electrode obtained at 450 and 700 °C, respectively; (c) is the cross-sectional SEM image of the TiO$_2$/BDD electrode; (d) is XRD patterns of the TiO$_2$/BDD electrode obtained at 700 °C (1) and 450 °C (2) and the pure BDD electrode (3)

XRD patterns were usually used to analyze the crystalline phase composition of the TiO$_2$/BDD obtained at different temperatures. Fig. 1d shows the XRD patterns of the TiO$_2$/BDD electrode obtained at 700 °C (curve 1), at 450 °C (curve 2) and pure BDD electrode (curve 3). The well-defined diamond peaks at 2θ degree of *ca*. 44° for curve 1 is almost identical to that for curve 3 in Fig. 1d, which further demonstrates that the physicochemical properties of the BDD were maintained through the above radical treatments. Another two distinctive diffraction peaks at 2θ degree of *ca*. 25.4 and 27.6° for curve 1 in Fig. 1d could be indexed to anatase-phase (JCPDS No. 21-1272) and rutile-phase (JCPDS No. 21-1276), respectively. The TiO$_2$/BDD film contained 93 % of anatase and 7 % of rutile according to the empirical relationship used by Depero *et al*.[22]. It suggests that the difference of substrates had no significant effect on the crystallinine phase of TiO$_2$.

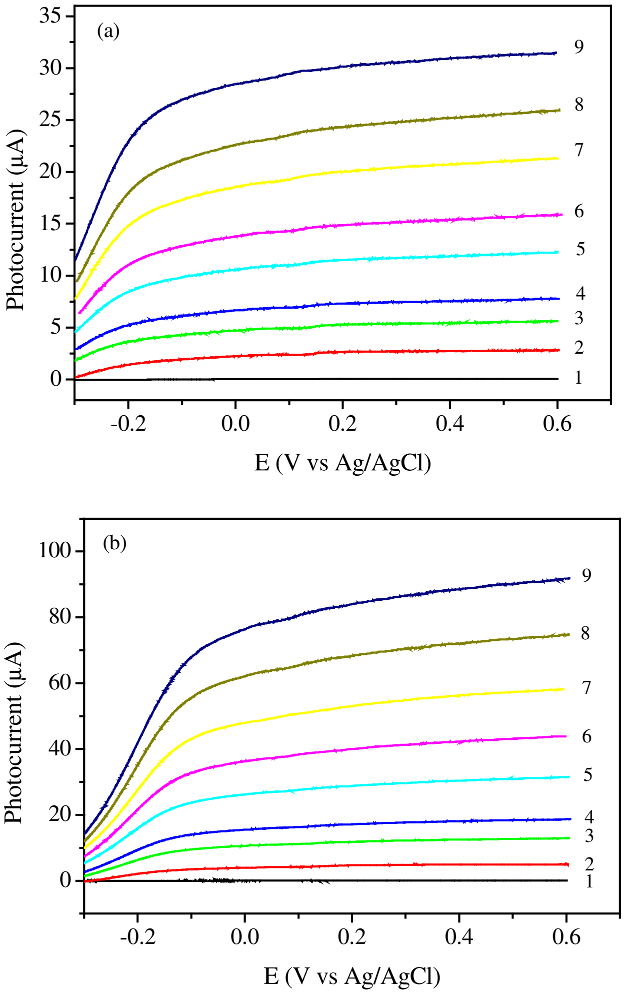

Fig. 2. Linear sweep voltammograms of TiO$_2$/BDD heterojunction electrode calcined at 450 °C (a) and 700 °C (b) obtained from 0.1 M NaNO$_3$ electrolyte solution under different light intensity, curve 1: in dark; the light intensity for curve 2-9 in turn were 0.6, 1.6, 2.3, 3.8, 4.9, 6.6, 8.1, 9.8 mW cm^{-2}

Photoelectrochemical characterization: The photocatalytic activity of TiO$_2$/BDD heterojunction electrode was subsequently investigated. The applied potential can effectively separate the photoelectrons and photoholes, to form the photocurrent. It is considered that the photocurrent is related to the light intensity. Therefore, the effects of potential bias and light intensity on photocurrent were investigated in this work. Fig. 2 shows the linear sweep voltammograms obtained at the TiO$_2$/BDD heterojunction electrode in 0.1 M NaNO$_3$ electrolyte solution with or without the UV illumination. The results revealed that without illumination only negligible dark current was obtained [curve 1 in Fig. 2(a-b)], which suggesting water cannot be directly decomposed by the potential bias applied. Curve 2-9 show the photocurrent response of the electrode with the different intensity of UV illumination. In all cases, the photocurrent increased with potential before levelling off to their own saturated photocurrent. From the linear sweep voltammograms, two aspects of information can be obtained. One is the increasing part of photocurrent (*i.e*., -0.3 V to -0.1 V), indicating that electron transport in the TiO$_2$/BDD electrode was the rate-limiting process which like a pure resistance in its response to the potential change. The other is the levelling off part (*i.e*., over -0.1 V), which is the kinetic information of photohole capture process at the TiO$_2$/BDD electrode/solution interface[23]. The amount of the saturated photocurrents can be used to quantitatively represent the photocatalytic activity of photocatalyst because it represents the maximum rate of oxidation under a given light intensity[17,23]. For all cases with UV illumination, it is found that the saturated photocurrents at the mixed-phase TiO$_2$/BDD electrode are 3-fold of that obtained at pure-anatase TiO$_2$/BDD electrode. Therefore, the photocatalytic activity of the mixed-phase TiO$_2$/BDD electrode is much higher than that at pure-anatase TiO$_2$/BDD electrode. This may be contributed to the mixed anatase and rutile phases occurred at 700 °C[17]. The relationship between saturation photocurrent and light intensity under two conditions was plotted in Fig. 3. The slope at the mixed-phase TiO_2/BDD electrode is almost 2 times higher than that at pure-anatase TiO_2/BDD electrode, further indicating an improved photocatalytic activity toward water oxidation. This may be also attributed to the mixed anatase/rutile phase coming into being at 700 ºC. Therefore, the following experiments were carried out at mixed-phase TiO_2/BDD electrode.

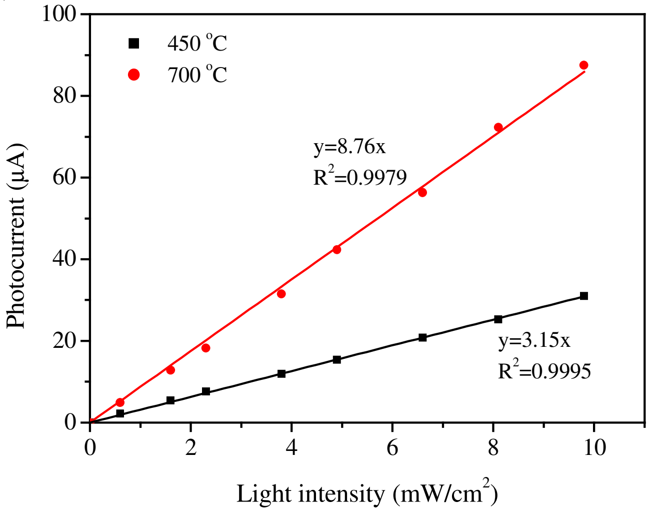

Fig. 3. Relationship between saturation photocurrent and light intensity

Optimization of detecting conditions

Potential bias: The effect of applied potential bias on photocurrent was investigated with or without the UV illumination, in 0.1 M $NaNO_3$ blank solution and various concentrations of glucose. No measurable current was observed for the blank and glucose solution without UV illumination, as shown curve 1 in Fig. 4, which suggesting water and/or glucose cannot be direct electrochemically decomposed in this potential range. However, as applied potential bias was increased up to a critical value under illumination, a linear increase of photocurrent was observed. Beyond the critical value, the photocurrent levelled off. These critical values of the potential bias were found to be between -0.18 and 0.1 V *versus* the Ag/AgCl reference electrode depending on the light intensity and the concentration of organics in the solution. To ensure the sufficient potential bias under various conditions while at the same time minimizing the direct electrochemical reaction, a potential bias of +0.40 V was selected for the detecting experiments.

Light intensity: The effect of light intensity was also investigated in a constant concentration of glucose (10 mM glucose in 0.1 M $NaNO_3$). Fig. 5 showed that the saturation photocurrent was directly proportional to the applied light intensity. Therefore, the detecting sensitivity is directly proportional to the light intensity employed. For this reason, a high light intensity should be expected. In practice, however, the high light intensity is often associated with stability problems, which may lead to the poor reproducibility. Hence, a relatively low light intensity of 6.6 mW cm^{-2} was selected in the following experiments.

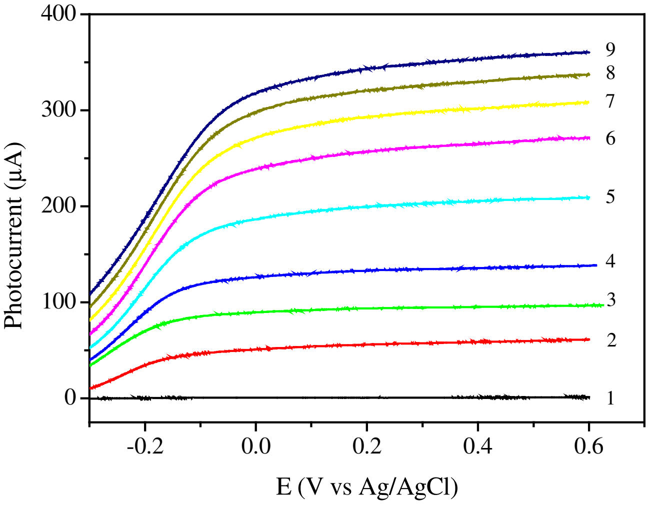

Fig. 4. Linear sweep voltammograms of mixed-phase TiO_2/BDD electrode obtained from 0.1 M $NaNO_3$ blank and working solution, Scanning rate is 5 mV/s; light intensity is 6.6 mW/cm^2. Curve 1: dark current. Curve 2-9 were obtained from the working solution under UV illumination; the concentration of glucose in turn were 0, 0.2, 0.4, 0.8, 1.5, 3.0, 6.0 and 10 mM

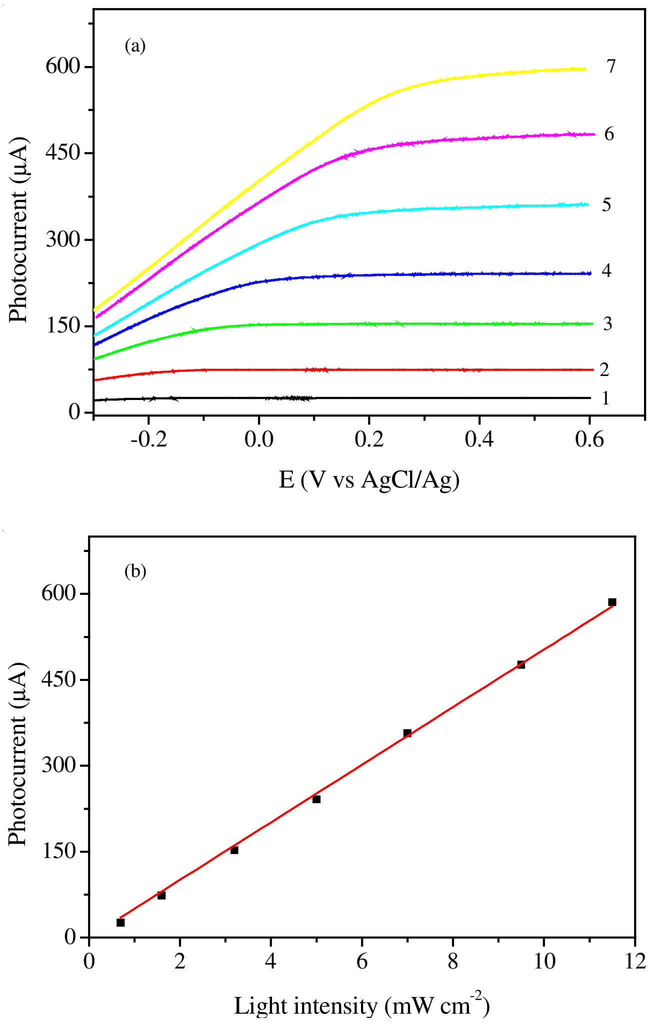

Fig. 5. (a) Linear sweep voltammograms of mixed-phase TiO_2/BDD electrode obtained from a solution containing 0.1 M $NaNO_3$ + 10 mM glucose under illumination of different light intensities. Curves 1-7 in turn were 0.7, 1.6, 3.2, 5.0, 7.0, 9.5, 11.5 mW cm^{-2} (measured at 365 nm). (b) The relationship between saturation photocurrent and light intensity

pH: The pH was considered as one of the important factors in the sensing process. It has influence on not only the form of compounds monitored but also the state of sensing elements. Therefore, the pH influence on the reaction rate and signal sensitivity was investigated in 0.1 M NaNO$_3$ at a constant potential bias of +0.4 V with illumination of 6.6 mW cm^{-2}. Fig. 6 showed that within the pH range of 2-10, the photocurrents for solutions with organic compounds and without organic compounds remained almost unchanged with pH. When pH was beyond 11, the blank and total photocurrents both fast increased, whereas the net photocurrent decreased, suggesting the photocatalytic activity of organic compounds was compressed. This trend is similar to that previously found in the TiO$_2$ films on ITO electrode where photocurrent of organic compounds had little influence by pH changes. Hence, pH was controlled in the range of 2-10 during analytical experiment of organic compounds.

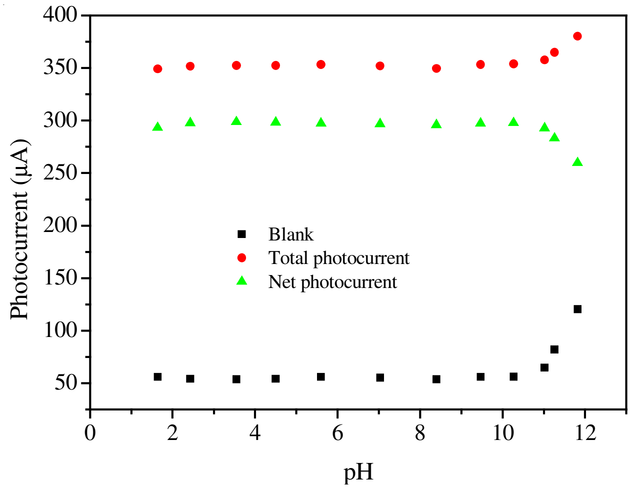

Fig. 6. Effect of pH on the saturation photocurrent of glucose (10 mM in 0.1 NaNO$_3$) at mixed-phase TiO$_2$/BDD electrode with illumination of 6.6 mW cm^{-2}

Chemical stability: To investigate the chemical stability during the practical application, the photocurrent after reduplicative dipping in the acidic (pH = 1.0) and basic (pH = 12.0) solution, each dipping was performed for 1 day, was examined. The results showed that the saturation photocurrent of mixed-phase TiO$_2$/BDD electrodes still keep at an almost constant rang from 58-55 µA after 10 cycles of investigating effect of pH, demonstrating that the mixed-phase TiO$_2$/BDD electrodes were strong acid and alkali resistant properties. This may be attributed to the acid and alkali resistance of BDD. For control purpose, the chemical stability of mixed-phase TiO$_2$/ITO electrodes was also performed under identical experimental conditions. The photocurrent at mixed-phase TiO$_2$/ITO electrodes dropped from 71.8 µA to almost zero after only one dipping cycle. It was visible observed that the TiO$_2$ layer peeled off. Therefore, the disappearance of photocurrent should be due to total deterioration of TiO$_2$, possibly induced by the damage of ITO in acidic and basic solution[24]. This indicated that the practical application of photoelectrochemical analysis of mixed-phase TiO$_2$/BDD electrodes is much broader than that of mixed-phase TiO$_2$/ITO electrodes.

Detection of organic compounds: The steady-state photocurrent values of glucose and KHP at mixed-phase TiO$_2$/BDD electrode under the constant potentials of 400 mV with illumination of 6.6 mW cm^{-2}, were examined. Fig. 7(a) showed a set of typical photocurrent-time profiles obtained in the presence and absence of organic compounds with illumination of light intensity of 6.6 mW cm^{-2} (365 nm) and without illumination at mixed-phase TiO$_2$/BDD electrode. Under a constant applied potential of +0.40 V, when the UV light was switched off, the dark current was approximately zero. Upon illumination, the current increased rapidly before decaying to a steady value. For the blank (curve 2 in Fig. 7), the photocurrent (i_{Blank}) resulted mainly from the oxidation of water, while photocurrent (i_{Total}) observed from the sample solution containing organics (curve 3 in Fig. 7) is the total current of two current components, one from the oxidation of water, which was the same as the blank photocurrent (i_{Blank}) and the other from photoelectrocatalytic oxidation of organic compounds. The net steady state current (i_{Net}), *i.e.*, the limiting current, originated from the oxidation of organics, can be obtained by subtracting the photocurrent of the blank (i_{blank}) from the total photocurrent. i_{net} was then used to quantify the concentration of organic compounds. The relationships between i_{net} and concentration for glucose and KHP were plotted in Fig. 7(b). It can be seen that for both organic compounds investigated, the i_{net} obtained were directly proportional to the concentration, suggesting that the mixed-phase TiO$_2$/BDD electrode can be effectively used for the detection of organic compounds.

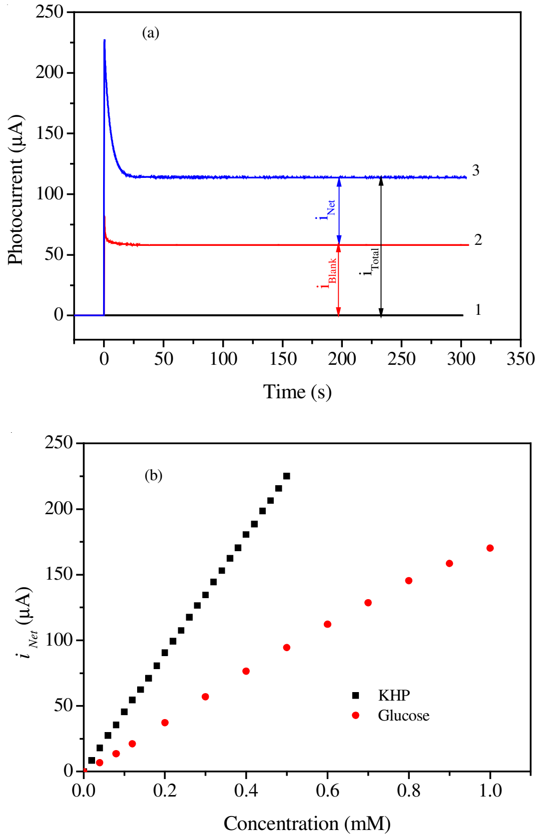

Fig. 7. (a) Typical photocurrent responses of 0.1 M NaNO$_3$ blank solution (2) and a 0.1 NaNO$_3$ solution containing organic compounds (3) with illumination and without illumination (1). (b) The relationship between photocurrent and concentration for glucose and KHP

Conclusion

In this work, the TiO_2/BDD heterojunction electrode was prepared using the simple dip-coating method. The mixed-phase TiO_2/BDD electrode has a high photoelectrocatalytic activity and a high resistance for acidic and alkali corrosion. Moreover, the photocurrent keeps almost constant in the pH range from 2-10. The i_{net} at a constant potential of +0.4 V is directly proportional to the concentration of organic compounds detected. These outstanding characteristics recommend this heterojunction electrode as an excellent sensing material for organic compounds.

ACKNOWLEDGEMENTS

The study was supported by the Key Laboratory of Industrial Ecology and Environmental Engineering (No. 0908) (Dalian University of Technology), China Ministry of Education, Funding Project for Academic Human Resources Development in Institutions of Higher Learning Under the Jurisdiction of Beijing Municipality (No. PHR201107213) and A Project Supported by Scientific Research Fund of Liaoning Provincial Education Department (No. L2010233).

REFERENCES

1. N. Mitani and Y. Einaga, *J. Electroanal. Chem.*, **626**, 156 (2009).
2. K.B. Holt, A.J. Bard, Y. Show and G.M. Swain, *J. Phys. Chem. B*, **108**, 15117 (2004).
3. W.C. Poh, K.P. Loh, W.D. Zhang, S. Triparthy, J.-S. Ye and F.-S. Sheu, *Langmuir*, **20**, 5484 (2004).
4. I. Sirés, E. Brillas, G. Cerisola and M. Panizza, *J. Electroanal. Chem.*, **613**, 151 (2008).
5. H. Yu, S. Chen, X. Quan, H. Zhao and Y. Zhang, *Environ. Sci. Technol.*, **42**, 3791 (2008).
6. R. Kalish, *Carbon*, **37**, 781 (1999).
7. B.P. Chaplin, I. Wyle, H. Zeng, J.A. Carlisle and J. Farrell, *J. Appl. Electrochem.*, **41**, 1329 (2011).
8. M.R. Hoffmann, S.T. Martin, W. Choi and D.W. Bahnemann, *Chem. Rev.*, **95**, 69 (1995).
9. X. Zhang, X. Zhao and H. Su, *Korean J. Chem. Eng.*, **28**, 1241 (2011).
10. H.-J. Jung, J.-S. Hong and J.-K. Suh, *Korean J. Chem. Eng.*, **28**, 1882 (2011).
11. H. Zhao, D. Jiang, S. Zhang, K. Catterall and R. John, *Anal. Chem.*, **76**, 155 (2004).
12. A. Fujishima and K. Honda, *Nature*, **238**, 37 (1972).
13. L. Andronic and A. Duta, *Mater. Chem. Phys.*, **112**, 1078 (2008).
14. D.M. Chen, D. Yang, J.Q. Geng, J.H. Zhu and Z.Y. Jiang, *Appl. Surf. Sci.*, **255**, 2879 (2008).
15. S.T. Han, J. Li, H.L. Xi, D.N. Xu, Y.J. Zuo and J.H. Zhang, *J. Hazard. Mater.*, **163**, 1165 (2009).
16. H.Y. He, *Int. J. Environ. Res.*, **3**, 57 (2009).
17. D. Jiang, S. Zhang and H. Zhao, *Environ. Sci. Technol.*, **41**, 303 (2007).
18. X. Li, L. Liu, Q. Meng and B. Cao, *J. Appl. Electrochem.*, **42**, 249 (2012).
19. A. Manivannan, N. Spataru, K. Arihara and A. Fujishima, *Electrochem. Solid-State Lett.*, **8**, C138 (2005).
20. J. Qu and X. Zhao, *Environ. Sci. Technol.*, **42**, 4934 (2008).
21. D. Jiang, H. Zhao, S. Zhang, R. John and G.D. Will, *J. Photochem. Photobiol. A*, **156**, 201 (2003).
22. L.E. Depero, L. Sangaletti, B. Allieri, E. Bontempi, R. Salari, M. Zocchi, C. Casale and M. Notaro, *J. Mater. Res.*, **13**, 1644 (1998).
23. D. Jiang, H. Zhao, S. Zhang and R. John, *J. Phys. Chem. B*, **107**, 12774 (2003).
24. J. Stotter, Y. Show, S. Wang and G. Swain, *Chem. Mater.*, **17**, 4880 (2005).